Available online at http://scik.org
Commun. Math. Biol. Neurosci. 2024, 2024:124
https://doi.org/10.28919/cmbn/8008
ISSN: 2052-2541

THE EFFECTIVENESS OF TRAVEL RESTRICTION AND VACCINATION FOR MULTI-REGION DISCRETE-TIME SIRI EPIDEMIC MODEL: OPTIMAL CONTROL APPROACH

SAMIRA ZOUHRI*, MOHCINE EL BAROUDI, HASSAN LAARABI

Laboratory of Analysis, Modeling, and Simulation (LAMS), Department of Mathematics and Computer Science, Hassan II University of Casablanca, Faculty of Sciences Ben M'sik, Sidi Othman, BP 7955, Casablanca, Morocco

Abstract. In this paper, we develop a multi-region discrete-time SIRI epidemic model, which describes the spatial-temporal spread of an infectious disease in a geographical domain divided into p regions and assumed to be connected and allow their people's mobility. We introduce two control variables into our model to study the effectiveness of travel restriction and vaccination in limiting the spread of epidemic. We aim to reduce the number of infected individuals in all regions and minimize the cost of administering travel ban and vaccination. In addition, we propose an optimal control approach using the definition of a supplementary function that identifies the activation of travel restriction and vaccination in every region according to health authority decisions. Numerical results are presented where we test the spread of epidemic without any intervention, when travel restriction only is applied, and when vaccination is added.

Keywords: discrete SIRI model; travel restriction; vaccination; multi-region; optimal control.

2020 AMS Subject Classification: 92D30.

*Corresponding author

E-mail address: samira.zouhrii@gmail.com

Received May 03, 2023

1. INTRODUCTION

The mathematical modeling of infectious disease is not a recent field of recherche; it was originally addressed by Daniel Bernoulli in the eighteenth century with his model on inoculation against the endemic smallpox. Over the years, the need to understand the disease's causes, to predict its evolution, and to develop methods to control its development has increased. Mathematical models has offered some response elements to scientists. In 1927, Kermack and Mckendrick proposed a simple mathematical model that estimates the potential number of infected individuals with a contagious disease in a closed community over time [1]. Their model, called the SIR model, consists of three components: susceptible (S), infected (I) and recovered (R). The susceptible component represents individuals who have never been infected, the infected component represents individuals who have been infected and can spread the disease, and the recovered component represents individuals who have been infected and recovered from the disease and assumed to have a permanent immunity.

Numerous works have proposed to mathematically analyzing infectious diseases, and several optimization strategies have been developed to control specific diseases [24, 25] such as ZIKA virus [2], HIV [3, 4] Malaria [5, 6], Tuberculosis [7, 8], COVID-19 [9, 10, 26], Ebola [11], the influenza pandemic [12] and others [13, 14]. One common factor between these infectious diseases is their capacity to spread from one place to another, and sometimes from one continent to another. This sheds light on the importance of disease spatial dynamics during the modeling process.

The modeling of infectious diseases spread require an approach that takes into account the spatial temporal evolution. In this case, modeling by partial differential equations (PDEs) is more appropriate. However, systems involving space and time variables turn out to be very complex to model and solve, and most of them are continuous, which contrasts with the nature of epidemic data collected in discrete time. Some researchers have proposed a discrete approach that makes it possible to escape the difficulties linked to the resolution and numerical manipulation of PDEs such as cellular automata (CA) [15, 16], Agent-based models (ABM) [17, 23] and an approach based on a multi-region SIR discrete-time model [18] where it is possible to model

the spread of epidemics from one region to another and to show the impact of travel from an infected region on another.

In this paper and based on the model [18], we develop a discrete time multi-region SIRI model that describes the spatiotemporal transmission of an infectious disease in a geographical domain divided into p regions and we add the assumption that removed individuals may relapse and become infected which is more complicated than the SIR case. We intend to control the spread of the epidemic and reduce the number of infected people in p regions. We consider two control functions corresponding to travel restriction and vaccination, and we aim to study their effectiveness and reduce the cost of their administration, as well as to determine when movement restrictions alone can reduce the spread of the epidemic, when travel ban alone is insufficient, and when vaccination intervention is required. We make sure that the interventions of travel ban and vaccination are automatically activated when a region is declared an infectious zone, which occurs when the number of infected individuals exceeds a high-risk threshold set by the health authorities. Since this intervention may happen in multiple regions at the same time, we develop a multi-objective optimization criteria that is subject to multi-point boundary value optimal control problem.

Our paper is organized as follows: Section 2 represents the discrete-time SIRI epidemic model with p regions. In Section 3 we introduce two control functions to the SIRI model and we characterize the optimal controls using a discrete version of Pontryagin's maximum principle then we derive the corresponding optimality system. Finaly, in Section 4 we presents our numerical results.

2. DISCRETE-TIME SIRI EPIDEMIC MODEL WITH p REGIONS

In this section we consider a discrete-time SIRI epidemic model in which the total host population is divided into three categories: susceptible (S), infected (I), and recovered (R), with the assumption that the immunity acquired following the recovery phase is not permanent, i.e., the individuals who have recovered from an infection may relapse and became infected. The interaction of different individuals from various classes will be studied within a specific domain $\mathscr{D}$, we assume that there are p connected regions (subdomains) inside $\mathscr{D}$ such that $\mathscr{D} = \bigcup_{i=1}^{p} \mathscr{D}_i$.

Let $S_k^{\mathscr{D}_i}$, $I_k^{\mathscr{D}_i}$, $R_k^{\mathscr{D}_i}$ are respectively the number of susceptible, infected and removed individuals who are present in the region $\mathscr{D}_i$ at time k. Individuals from the three compartments may be born, die, or change their compartment between the times k and $k+1$. The individuals in the susceptible compartment could stay susceptible, become infected and move to the infected compartment, or pass away (natural death). The individuals in the infected compartment can remain infected or get recovered and move to the recovered compartment or pass away. The individuals in the recovered compartment may stay there or move to the infected compartment or die.

Based on the same modeling assumptions in [18, 19, 20], it is assumed that:

i) There is constant recruitment, by birth and immigration, to the susceptible class .
ii) The birth and death happen at the same rate.
iii) Birth occurs in the home region at a rate of $d > 0$, as individuals who are outside their region do not give birth. And death happens anywhere at a rate of d.
iv) It is assumed that there is no infection-related mortality.

Let $N_k^{\mathscr{D}_i} = S_k^{\mathscr{D}_i} + I_k^{\mathscr{D}_i} + R_k^{\mathscr{D}_i}$ be the total number of individuals present in the region $\mathscr{D}_i$ at time k. Assume that the total number of individuals corresponding to the region $\mathscr{D}_i$ is fixed, that is, $N_{k+1}^{\mathscr{D}_i} = N_k^{\mathscr{D}_i}$, for all $k \geq 0$.

The disease transmission in a given region $\mathscr{D}_i$ at time k is given by: $\sum_{j=1}^{p} \beta_{ij} \frac{I_k^{\mathscr{D}_j}}{N_k^{\mathscr{D}_i}} S_k^{\mathscr{D}_i}$ Where $\beta_{ij} > 0$ is the contact rate in region $\mathscr{D}_i$ between susceptible and infected individuals from $\mathscr{D}_i$ or susceptible individual from $\mathscr{D}_i$ and infected individual from another region $\mathscr{D}_j$.

The evolution of the number of susceptible, infected and removed individuals in a given region $\mathscr{D}_i$ is as follows:

$$
(1) \qquad \begin{cases} S_{k+1}^{\mathscr{D}_i} = S_k^{\mathscr{D}_i} - \sum_{j=1}^{p} \beta_{ij} \frac{I_k^{\mathscr{D}_j}}{N_k^{\mathscr{D}_i}} S_k^{\mathscr{D}_i} + \left(N_k^{\mathscr{D}_i} - S_k^{\mathscr{D}_i} \right) d_i \\ I_{k+1}^{\mathscr{D}_i} = I_k^{\mathscr{D}_i} + \sum_{j=1}^{p} \beta_{ij} \frac{I_k^{\mathscr{D}_j}}{N_k^{\mathscr{D}_i}} S_k^{\mathscr{D}_i} - (\alpha_i + d_i) I_k^{\mathscr{D}_i} + \gamma_i R_k^{\mathscr{D}_i} \\ R_{k+1}^{\mathscr{D}_i} = R_k^{\mathscr{D}_i} + \alpha_i I_k^{\mathscr{D}_i} - (\gamma_i + d_i) R_k^{\mathscr{D}_i} \end{cases}
$$

Where $k = 0, 1, ..., T-1$, T is the final time, d_i is the birth and the natural death rate, α_i is the recovery rate, γ_i is the rate at which recovered individuals lose their immunity and return to the infected compartment. It is noticeable that $\gamma_i = 0$ implies that the recovered individuals acquire permanent immunity, which means that the individuals in the recovered class don't leave the compartment, in this case we are referring to the SIR epidemic model. All these parameters are associated to a given region D_i.

3. Optimal Control Approach: Travel Restriction and Vaccination

In this section, we use optimal control theory to minimize the number of infected individuals, travel restriction and vaccination cost at each region $\mathscr{D}_i$ which has been declared infectious area. We introduce into the model (1) two control variables $u_k^{\mathscr{D}_i}$ and $v_k^{i\mathscr{D}_j}$, which characterize respectively the vaccination intervention and the travel restriction that prevents other infected individuals from traveling from their initial regions with high risk of infection $\mathscr{D}_j$ and being in contact with susceptible individuals in the region $\mathscr{D}_i$. The authorities usually take time to determine the viral diagnostics and preventive techniques, to monitor and track the disease before classifying a region as an infectious zone and restricting people's movement. In addition, the infectious disease vaccination is not immediately available, especially when the disease has never been seen before. The development of a suitable vaccine takes also time. We assume that each region with an infected number that exceeds an agreed-upon threshold $\mathscr{T}$ for high risk, as determined by the health authorities, is declared as infectious, and it will be accessible for public health intervention via travel ban and vaccination. For this reason, we define a boolean variable δ_i associated to the region $\mathscr{D}_i$ and refers to the activation of the authority's travel ban restriction and vaccination. $\delta_i = 1$ means that the number of infected individuals in region $\mathscr{D}_i$ at time k exceeds $\mathscr{T}$, and thus travel restriction and vaccination are applied on this region. We can define the boolean variable δ_i such that:

$$\delta_i = \begin{cases} 0 & I_k^{\mathscr{D}_i} < \mathscr{T} \\ 1 & I_k^{\mathscr{D}_i} \geqslant \mathscr{T} \end{cases}$$

Taking into account all of these factors, for a given region $\mathscr{D}_i$, the model with control terms is as follows:

$$
(2)\qquad \begin{cases} S_{k+1}^{\mathscr{D}_i} = S_k^{\mathscr{D}_i} - \sum_{j=1}^{p} \left(1 - \delta_i v_k^{i\mathscr{D}_j}\right) \beta_{ij} \frac{I_k^{\mathscr{D}_j}}{N_k^{\mathscr{D}_i}} S_k^{\mathscr{D}_i} + \left(N_k^{\mathscr{D}_i} - S_k^{\mathscr{D}_i}\right) d_i - \delta_i u_k^{\mathscr{D}_i} S_k^{\mathscr{D}_i} \\ I_{k+1}^{\mathscr{D}_i} = I_k^{\mathscr{D}_i} + \sum_{j=1}^{p} \left(1 - \delta_i v_k^{i\mathscr{D}_j}\right) \beta_{ij} \frac{I_k^{\mathscr{D}_j}}{N_k^{\mathscr{D}_i}} S_k^{\mathscr{D}_i} - (\alpha_i + d_i) I_k^{\mathscr{D}_i} + \gamma_i R_k^{\mathscr{D}_i} \\ R_{k+1}^{\mathscr{D}_i} = R_k^{\mathscr{D}_i} + \alpha_i I_k^{\mathscr{D}_i} - (\gamma_i + d_i) R_k^{\mathscr{D}_i} + \delta_i u_k^{\mathscr{D}_i} S_k^{\mathscr{D}_i} \end{cases}
$$

We can see that when $\delta_i = 1$, $u_k^{\mathscr{D}_i} S_k^{\mathscr{D}_i}$ individuals move from the susceptible compartment to the removed one at time k in region $\mathscr{D}_i$, so the control $u_k^{\mathscr{D}_i}$ may be interpreted as the proportion of individuals to be vaccinated. Our goal is to minimize our objective functional:

$$
(3)\qquad J(u,v) = \sum_{j=1}^{p} \delta_i J_j(u^{\mathscr{D}_j}, v^{j\mathscr{D}})
$$

where $J_j(u^{\mathscr{D}_j}, v^{j\mathscr{D}})$ is defined by:

$$
(4)\qquad J_i(u^{\mathscr{D}_i}, v^{i\mathscr{D}}) = I_T^{D_i} + \sum_{l \in O} \sum_{k=0}^{T-1} \left(I_k^{D_i} + \delta_i A_i \left(u_k^{\mathscr{D}_i}\right)^2 + \delta_i B_i \left(v_k^{i\mathscr{D}_l}\right)^2 \right)
$$

Where $\mathscr{O} = \{l \in [\![1..p]\!] \mid \delta_l = 1\}$ is the set of indices of regions declared infectious. $A_i > 0$ and $B_i > 0$ are the weight factors of controls, with $u = \left(u^{\mathscr{D}_1}, ..., u^{\mathscr{D}_p}\right)$ and $v = \left(v^{1\mathscr{D}}, ..., v^{p\mathscr{D}}\right)$, where $u^{\mathscr{D}_i} = \left(u_0^{\mathscr{D}_i}, ..., u_{T-1}^{\mathscr{D}_i}\right)$ and $v^{i\mathscr{D}_l} = \left(v_0^{i\mathscr{D}_l}, ..., v_{T-1}^{i\mathscr{D}_l}\right)$.

We aim to minimize the number of infected individuals, in each region $\mathscr{D}_i$ declared infectious, during the time steps $k = 1$ to $k = T-1$ and at the final time, as well as to reduce the cost of administering the controls. We seek a pair of control (u,v) which minimizes the objective functional:

$$
(5)\qquad J(u^*, v*) = \min\{J(u,v) : u \in \mathscr{U} \text{ and } v \in \mathscr{V}\}
$$

With $\mathscr{U}$ and $\mathscr{V}$ denote the control sets given by :

$$
\mathscr{U} = \left\{ u \text{ measurable}, \ u_{min}^{\mathscr{D}_i} \leq u_k^{\mathscr{D}_i} \leq u_{max}^{\mathscr{D}_i} \right\}
$$

$$
\mathscr{V} = \left\{ v \text{ measurable}, \ v_{min}^{i\mathscr{D}_l} \leq v_k^{i\mathscr{D}_l} \leq v_{max}^{i\mathscr{D}_l} \right\}
$$

where $k = 0, ..., T-1$ and $l \in \mathscr{O}$ and $0 < u_{min}^{\mathscr{D}_i} < u_{max}^{\mathscr{D}_i} < 1$ and $0 < v_{min}^{i\mathscr{D}_l} < v_{max}^{i\mathscr{D}_l} < 1$. Our optimal control problem can be solved using the Pontryagin's maximum principle. First, we determine

the Hamiltonian as follow:

$$
\begin{aligned}
H = & \sum_{k'=1}^{p} \delta_{k'} \left(\sum_{l \in \mathscr{O}} I_k^{D_{k'}} + \delta_{k'} A_{k'} \left(u_k^{\mathscr{D}_{k'}} \right)^2 + \delta_{k'} B_{k'} \left(v_k^{k' \mathscr{D}_l} \right)^2 \right) \\
& + \sum_{i=1}^{p} \delta_i \left(\varphi_{1,k+1}^i \left[S_k^{\mathscr{D}_i} - \sum_{j=1}^{p} \left(1 - \delta_i v_k^{i\mathscr{D}_j} \right) \beta_{ij} \frac{I_k^{\mathscr{D}_j}}{N_k^{\mathscr{D}_i}} S_k^{\mathscr{D}_i} + \left(N_k^{\mathscr{D}_i} - S_k^{\mathscr{D}_i} \right) d_i - \delta_i u_k^{\mathscr{D}_i} S_k^{\mathscr{D}_i} \right] \right. \\
& + \varphi_{2,k+1}^i \left[I_k^{\mathscr{D}_i} + \sum_{j=1}^{p} \left(1 - \delta_i v_k^{i\mathscr{D}_j} \right) \beta_{ij} \frac{I_k^{\mathscr{D}_j}}{N_k^{\mathscr{D}_i}} S_k^{\mathscr{D}_i} - (\alpha_i + d_i) I_k^{\mathscr{D}_i} + \gamma_i R_k^{\mathscr{D}_i} \right] \\
& \left. + \varphi_{3,k+1}^i \left[R_k^{\mathscr{D}_i} + \alpha_i I_k^{\mathscr{D}_i} - (\gamma_i + d_i) R_k^{\mathscr{D}_i} + \delta_i u_k^{\mathscr{D}_i} S_k^{\mathscr{D}_i} \right] \right)
\end{aligned} \tag{6}
$$

Where $j \in \mathscr{O}$

Theorem 1. *Let $u_k^{\mathscr{D}_i *}$ and $v_k^{\mathscr{D}_l *}$ be optimal controls, and $S^{\mathscr{D}_i *}$, $I^{\mathscr{D}_i *}$ and $R^{\mathscr{D}_i *}$ are solutions of the corresponding state system (1), there exists adjoint functions $\varphi_{q,k}^i$ with $k = 0, .., T-1$, $q \in [\![1,3]\!]$, satisfying the following equations:*

$$
\begin{cases}
\Delta \varphi_{1,k}^i = -\delta_i \left(\varphi_{1,k+1}^i \left[1 - \sum_{j=1}^{p} \left(1 - \delta_i v_k^{i\mathscr{D}_j} \right) \beta_{ij} \frac{I_k^{\mathscr{D}_j}}{N_k^{\mathscr{D}_i}} - d_i - \delta_i u_k^{\mathscr{D}_i} \right] \right. \\
\qquad \left. + \varphi_{2,k+1}^i \left[\sum_{j=1}^{p} \left(1 - \delta_i v_k^{i\mathscr{D}_j} \right) \beta_{ij} \frac{I_k^{\mathscr{D}_j}}{N_k^{\mathscr{D}_i}} \right] + \varphi_{3,k+1}^i \left[\delta_i u_k^{\mathscr{D}_i} \right] \right) \\
\Delta \varphi_{2,k}^i = -\delta_i \left(1 + \beta_{jj} \frac{1}{N_k^{\mathscr{D}_i}} S_k^{\mathscr{D}_i} \left[\varphi_{2,k+1}^i - \varphi_{1,k+1}^i \right] + (1 - \alpha_i - d) \varphi_{2,k+1}^i \right. \\
\qquad \left. + \varphi_{3,k+1}^i \alpha_i \right) \\
\Delta \varphi_{3,k}^i = -\delta_i \left(\varphi_{2,k+1}^i \gamma_i + \varphi_{3,k+1}^i (1 - \gamma_i - d_i) \right)
\end{cases} \tag{7}
$$

Where $\varphi_{1,T}^i = 0$, $\varphi_{2,T}^i = 1$ and $\varphi_{3,T}^i = 0$ are the transversality conditions for $i = 1, ..., p$.

In addition, our optimal controls

$u^* = \left(u^{\mathscr{D}_1 *}, ..., u^{\mathscr{D}_p *} \right)$ and $v^* = \left(v^{1\mathscr{D} *}, ..., v^{p\mathscr{D} *} \right)$.

where $u^{\mathscr{D}_i *} = \left(u_0^{\mathscr{D}_i *}, ..., u_{T-1}^{\mathscr{D}_i *} \right)$ and $v^{i\mathscr{D} *} = \left(v_0^{i\mathscr{D}_l *}, ..., v_{T-1}^{i\mathscr{D}_l *} \right)$, with $l \in \mathscr{O}$, are given by:

$$
u_k^{\mathscr{D}_i *} = \min \left(\max \left(u_{min}^{\mathscr{D}_i}, \delta_i \frac{\left(\varphi_{1,k+1}^i - \varphi_{3,k+1}^i \right) S_k^{\mathscr{D}_{i*}}}{2A_i} \right), u_{max}^{\mathscr{D}_i} \right), \text{ if } \delta_i = 1
$$

$$u_k^{\mathscr{D}_i*} = 0 \; if \; \delta_i = 0$$

$$v_k^{i\mathscr{D}_l*} = \min\left(\max\left(v_{min}^{i\mathscr{D}_l}, \delta_i \frac{\left(\varphi_{1,k+1}^i - \varphi_{2,k+1}^i\right)\beta_{il} I_k^{\mathscr{D}_l*} S_k^{\mathscr{D}_i*}}{2B_i N_k^{\mathscr{D}_i}}\right), v_{max}^{i\mathscr{D}_l}\right), \; if \; \delta_i = 1$$

$$v_k^{i\mathscr{D}_l*} = 0, \; if \; \delta_i = 0$$

Proof. We can obtain the adjoint equations using Pontryagin's Maximum Principle[21] as follows:

$$\Delta\varphi_{1,k}^i = -\frac{\partial H}{\partial S_k^{\mathscr{D}_i}}$$

$$\Delta\varphi_{2,k}^i = -\frac{\partial H}{\partial I_k^{\mathscr{D}_i}}$$

$$\Delta\varphi_{3,k}^i = -\frac{\partial H}{\partial R_k^{\mathscr{D}_i}}$$

Where $\varphi_{1,T}^i = 0$, $\varphi_{2,T}^i = 1$ and $\varphi_{3,T}^i = 0$ are the transversality conditions for $i = 1, ..., p$

To derive the optimality equations, we take the variation with respect to $u_k^{\mathscr{D}_i}$ and $v_k^{i\mathscr{D}_l}$, with:

$$\frac{\partial H}{\partial u_k^{\mathscr{D}_i}} = 0 \; at \; u_k^{\mathscr{D}_i*}$$

$$\frac{\partial H}{\partial v_k^{i\mathscr{D}_l}} = 0 \; at \; v_k^{i\mathscr{D}_l*}$$

as well, by taking controls bounds from $\mathscr{U}$ and $\mathscr{V}$ we obtain:

$$u_k^{\mathscr{D}_i*} = \min\left(\max\left(u_{min}^{\mathscr{D}_i}, \delta_i \frac{\left(\varphi_{1,k+1}^i - \varphi_{3,k+1}^i\right) S_k^{\mathscr{D}_i*}}{2A_i}\right), u_{max}^{\mathscr{D}_i}\right), if \; \delta_i = 1$$

$$v_k^{i\mathscr{D}_l*} = \min\left(\max\left(v_{min}^{i\mathscr{D}_l}, \delta_i \frac{\left(\varphi_{1,k+1}^i - \varphi_{2,k+1}^i\right)\beta_{il} I_k^{\mathscr{D}_l*} S_k^{\mathscr{D}_i*}}{2B_i N_k^{\mathscr{D}_i}}\right), v_{max}^{i\mathscr{D}_l}\right), if \; \delta_i = 1$$

□

Parameter	Description
β_{ij}	the contact rate
d_i	the birth and the natural death rate
α_i	the recovery rate
γ_i	the immunity lose rate

TABLE 1. Description of parameter model

region	S_0	I_0	R_0	β_{ij}	d_i	α_i	γ_i
$\mathscr{D}_1$	8000	40	50	0.065	0.16	0.001	0.01
$\mathscr{D}_2$	10000	900	80	0.065	0.16	0.001	0.01
$\mathscr{D}_3$	7000	50	40	0.065	0.16	0.001	0.01
$\mathscr{D}_4$	9000	900	30	0.065	0.16	0.001	0.01

TABLE 2. Parameter values and initial conditions associated to the 4 regions

4. NUMERICAL RESULTS

The standard Forward-Backward sweep method (FBSM) [22], which is still applicable in this discrete time scenario, can be used to solve our optimal control problem. This approach aims to solve the state system (1) forward in time using an initial guess and solve the adjoint system (9) backward in time. At each time step k, the stored values of the state and adjoint state variables are used to characterize the optimal controls $u_k^{\mathscr{D}_i *}$ and $v_k^{i\mathscr{D}_l *}$.

We choose the discrete-time SIRI epidemic model with $p = 4$ regions, $\mathscr{D} = \bigcup_{i=1}^{4} \mathscr{D}_i$ with different parameters as it is mentioned in table 1. $\mathscr{D}_2$ and $\mathscr{D}_4$ are presumed to be the infectious regions ($I_0^{\mathscr{D}_2} = 900$ and $I_0^{\mathscr{D}_4} = 900$) that call for vaccination and travel restrictions once their number of infected individuals reaches the threshold $\mathscr{T} = 1000$. $i = 0$ represents the first authority step to determine the viral diagnostics and preventive techniques and to monitor and track the disease before classifying a region as an infectious zone and restricting people's movement. Once $\mathscr{D}_2$ and $\mathscr{D}_4$ become infectious zone, the travel ban blocks the movement between regions $\mathscr{D}_2 \not\Rightarrow \mathscr{D}_4$ and $\mathscr{D}_4 \not\Rightarrow \mathscr{D}_2$. After that we wait for the other infectious zone to appear; if it does, the travel ban prevents people from moving between $\mathscr{D}_2 \not\Rightarrow \mathscr{D}_1$ and between $\mathscr{D}_4 \not\Rightarrow \mathscr{D}_3$.

Figure 1 (a) represents the state variables of the SIRI model in four regions without control. We can observe that the number of susceptible individuals in four regions decreases from $S_0^{\mathscr{D}_1} = 8000$, $S_0^{\mathscr{D}_2} = 10000$, $S_0^{\mathscr{D}_3} = 7000$ and $S_0^{\mathscr{D}_4} = 9000$ to 4450, 6896, 3696, and 6000 respectively, values that are still large. Figure 1 (b) shows the evolution of infected individuals in the four regions. We can see that the number of infected individuals increases remarkably from $I_0^{\mathscr{D}_1} = 40$, $I_0^{\mathscr{D}_2} = 900$, $I_0^{\mathscr{D}_3} = 50$ and $I_0^{\mathscr{D}_4} = 900$ to 3587, 4062, 3376, and 3909 respectively. We can observe that the regions $\mathscr{D}_2$ and $\mathscr{D}_4$ reached the high risk threshold at time $k = 10$ while the

regions $\mathscr{D}_1$ and $\mathscr{D}_3$ reached immediately after $\mathscr{D}_1$ and $\mathscr{D}_3$ the high risk threshold at time $k = 15$ due to the absence of any control. Figure 1 (c) shows the evolution of the removed individuals' number over time in the four regions. The number of removed individuals decreases and reaches a low number in each of the four regions.

We can deduce that in the lack of effective control, the epidemic may spread and cause dangerous damage.

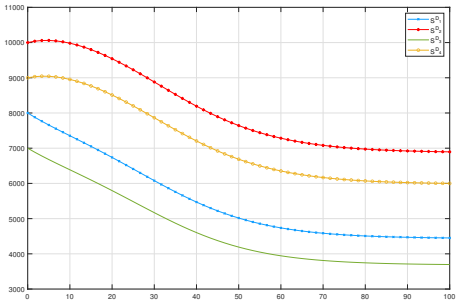

(A) Shape of state variable S associated to the regions $\mathscr{D}_1$, $\mathscr{D}_2$, $\mathscr{D}_3$ and $\mathscr{D}_4$

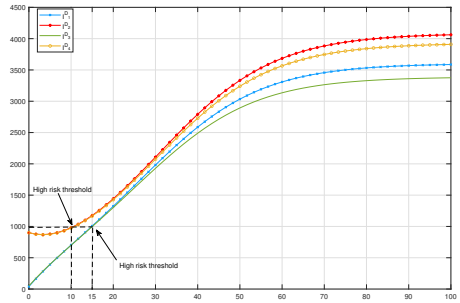

(B) Shape of state variable I associated to the regions $\mathscr{D}_1$, $\mathscr{D}_2$, $\mathscr{D}_3$ and $\mathscr{D}_4$

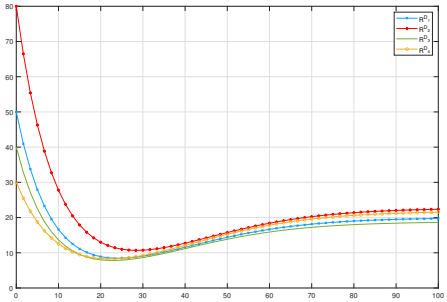

(C) Shape of state variable R associated to the regions $\mathscr{D}_1$, $\mathscr{D}_2$, $\mathscr{D}_3$ and $\mathscr{D}_4$

FIGURE 1. Temporal evolution of the state variables of the SIRI model in four regions without control

In Figure 2 (a), the travel restriction alone ($u = 0$) is applied where $\mathscr{T} = 500$. We can see that the number of infected individuals in four regions is remarkably decreased compared with the case when no control. Figure 2 (b) and (c) show the evolution of susceptible and recovered individuals during the application of travel restriction only. The number of susceptible

decreases in four regions from the start of travel ban until $k = 87$ and then starts to increase until the end of period which indicates that there is a contact between susceptible and infected individuals. While the number of recovered individuals reach low value in four regions, this may be explain by the fact that recovered individual not acquire a permanent immunity and can become infected.

In this case, the strategy of travel restriction only where $\mathscr{T} = 500$ has helped to reduce the number of infection in four regions, however it is not sufficient to attain a promising epidemiological situation especially since the four regions remain infectious until the end of time.

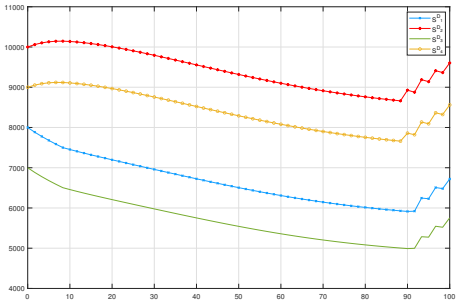

(A) Shape of state variable S associated to the regions $\mathscr{D}_1$, $\mathscr{D}_2$, $\mathscr{D}_3$ and $\mathscr{D}_4$

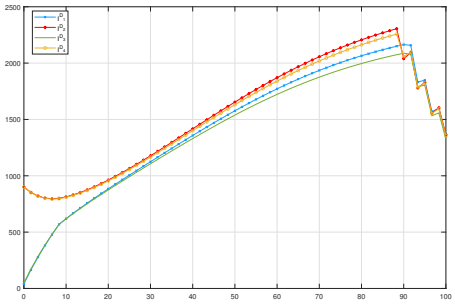

(B) Shape of state variable I associated to the regions $\mathscr{D}_1$, $\mathscr{D}_2$, $\mathscr{D}_3$ and $\mathscr{D}_4$

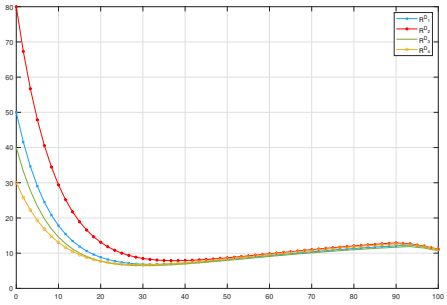

(C) Shape of state variable R associated to the regions $\mathscr{D}_1$, $\mathscr{D}_2$, $\mathscr{D}_3$ and $\mathscr{D}_4$

FIGURE 2. Temporal evolution of the state variables of the SIRI model in four regions with travel restriction only where $\mathscr{T} = 500$

Figure 3 (a) (b) (c) illustrates the results when a travel restriction is applied alone for $\mathscr{T} = 1000$. It is noticed that the number of infected individuals grows and reaches a high level, while the number of recovered people take a low value and the number of susceptible remains high. Travel restriction alone is not suitable when the number of infections is high, especially when removed individuals may relapse and become infected.

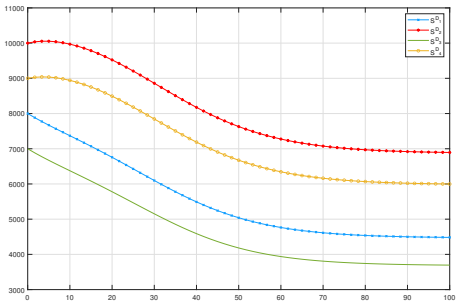

(A) Shape of state variable S associated to the regions $\mathscr{D}_1$, $\mathscr{D}_2$, $\mathscr{D}_3$ and $\mathscr{D}_4$

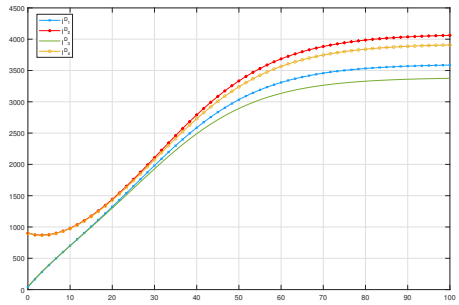

(B) Shape of state variable I associated to the regions $\mathscr{D}_1$, $\mathscr{D}_2$, $\mathscr{D}_3$ and $\mathscr{D}_4$

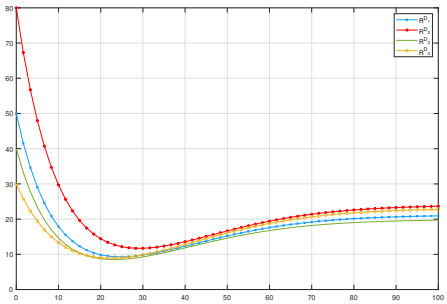

(C) Shape of state variable R associated to the regions $\mathscr{D}_1$, $\mathscr{D}_2$, $\mathscr{D}_3$ and $\mathscr{D}_4$

FIGURE 3. Temporal evolution of the state variables of the SIRI model in four regions with travel restriction only where $\mathscr{T} = 1000$

Figure 4 shows the evolution of susceptible, infected and removed individuals when travel restriction and vaccination are applied together for $\mathscr{T} = 1000$, the case for which the travel ban alone was not sufficient to give good results. As seen in Figure 4 (a), the reduction in the number of infected people is more significant than the case of travel restrictions alone. We

can see that after $k = 22$, the four regions have passed the high risk stage ($\mathscr{T} < 1000$), and at $k = 50$, the number of infected individuals appears to be nearly constant, with a slow decrease at the end of time. We can see in Figure 4 (b) that the number of susceptible individuals has remarkably reduced in four regions, starting with $S_0^{\mathscr{D}_1} = 8000$, $S_0^{\mathscr{D}_2} = 10000$, $S_0^{\mathscr{D}_3} = 7000$ and $S_0^{\mathscr{D}_4} = 9000$ and reaching $S^{\mathscr{D}_1} = 1928$, $S^{\mathscr{D}_2} = 2627$, $S^{\mathscr{D}_3} = 1684$ and $S^{\mathscr{D}_4} = 2374$ at the end of time and remain stagnant between $k = 20$ and $k = 100$. While the number of recovered people rises very quickly and reaches high value in four regions and remain constant between $k = 20$ and $k = 100$ as it is mentioned in figure 4 (c).

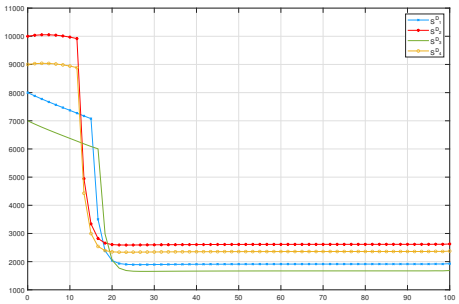

(A) Shape of state variable S associated to the regions $\mathscr{D}_1$, $\mathscr{D}_2$, $\mathscr{D}_3$ and $\mathscr{D}_4$

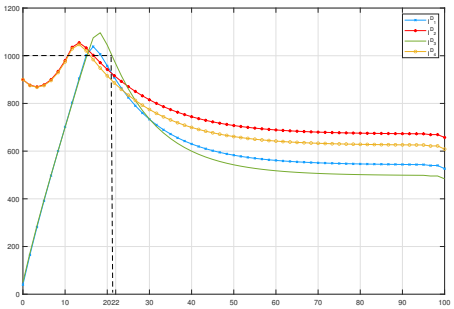

(B) Shape of state variable I associated to the regions $\mathscr{D}_1$, $\mathscr{D}_2$, $\mathscr{D}_3$ and $\mathscr{D}_4$

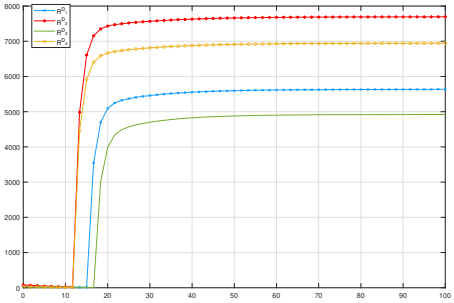

(C) Shape of state variable R associated to the regions $\mathscr{D}_1$, $\mathscr{D}_2$, $\mathscr{D}_3$ and $\mathscr{D}_4$

FIGURE 4. Temporal evolution of the state variables of the SIRI model in four regions with travel restriction and vaccination where $\mathscr{T} = 1000$

Figure 5 represents the controls $v^{1\mathscr{D}_2}$, $v^{2\mathscr{D}_4}$, $v^{3\mathscr{D}_4}$ and $v^{4\mathscr{D}_2}$ applied in regions $\mathscr{D}_1$, $\mathscr{D}_2$, $\mathscr{D}_3$ and $\mathscr{D}_4$ respectively. The four controls starts with value 0 which means that there is no travel ban

until that the region is declared infectious $\mathscr{T}_i >= 1000$ for $i = 1..4$. The optimal strategy in the four regions suggests starting with a small value of 0.2, which refers to low contact between infected and susceptible individuals from the different regions. The travel restriction remains strict until $k = 97$, where the four controls take values that exceed 0.5, which signifies that the travel restriction effect starts to decline allowing contact.

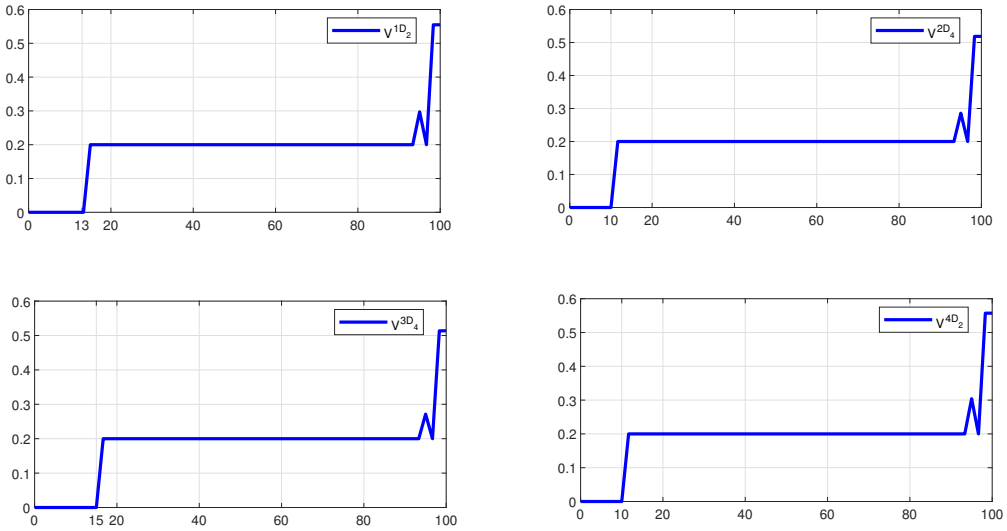

FIGURE 5. Shape of the travel restriction control associated to the regions $\mathscr{D}_1$, $\mathscr{D}_2$, $\mathscr{D}_3$ and $\mathscr{D}_4$

Figure 6 represents the controls $u^{\mathscr{D}_1}$, $u^{\mathscr{D}_2}$, $u^{\mathscr{D}_3}$ and $u^{\mathscr{D}_4}$ applied in regions $\mathscr{D}_1$, $\mathscr{D}_2$, $\mathscr{D}_3$ and $\mathscr{D}_4$ respectively. The vaccination strategy aims to vaccine an important proportion of individuals once the region has declared infectious until the end of time.

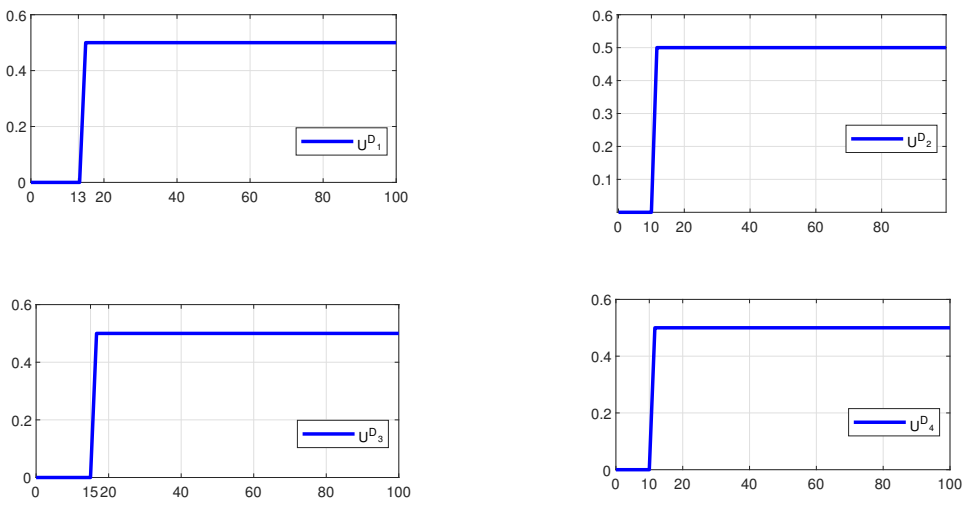

FIGURE 6. Shape of the vaccination control associated to the regions $\mathscr{D}_1$, $\mathscr{D}_2$, $\mathscr{D}_3$ and $\mathscr{D}_4$

According to our simulation results, travel restrictions alone can reduce the number of infected people when the high-risk threshold is not high ($\mathscr{T}_i = 500$). When it becomes large enough, the travel ban no longer works, especially in our case of non-permanent immunity. When travel restriction is applied with vaccination, even with a high risk threshold $\mathscr{T}_i = 1000$, this strategy has reduced the number of infection to under 650 cases in four regions and allowed to get rid of the infectious state in the four regions.

CONCLUSION

In this work, we develop a multi-region discrete-time SIRI epidemic model that represents the spatial-temporal transmission of an infectious disease in a geographical domain separated into p regions. In order to control the epidemic spread in each region and to optimize more than one objective function simultaneously, we formulate multi-objective optimization criteria. We add to the model two control functions that describe the intervention of travel restriction and vaccination in each region. This intervention is carried out in accordance with official decisions. Due to this, we developed a new function to specify the regions in which the travel ban and vaccine requirements will be implemented. The multi-point boundary value problems related

to our optimal control problem is obtained using a discrete version of Pontryagin's maximum principle. Our numerical results show that travel restriction alone can reduce the number of infected people when the number of infections is not high (high risk threshold $\mathscr{T}_i = 500$). The effectiveness of travel ban increases with how quickly it is implemented. When $\mathscr{T}_i = 1000$ travel ban alone is not effective; however, when combined with vaccination, we obtain good results.

CONFLICT OF INTERESTS

The authors declare that there is no conflict of interests.

REFERENCES

[1] W.O. Kermack, A.G. McKendrick, A contribution to the mathematical theory of epidemics, Proc. R. Soc. Lond. Ser. A. 115 (1927), 700–721. https://doi.org/10.1098/rspa.1927.0118.

[2] C. Ding, N. Tao, Y. Zhu, A mathematical model of Zika virus and its optimal control, in: 2016 35th Chinese Control Conference (CCC), IEEE, Chengdu, China, 2016: pp. 2642–2645. https://doi.org/10.1109/ChiCC.2016.7553763.

[3] M. Roshanfekr, M.H. Farahi, R. Rahbarian, A different approach of optimal control on an hiv immunology model, Ain Shams Eng. J. 5 (2014), 213–219. https://doi.org/10.1016/j.asej.2013.05.004.

[4] Y. Zhou, Y. Liang, J. Wu, An optimal strategy for HIV multitherapy, J. Comput. Appl. Math. 263 (2014), 326–337. https://doi.org/10.1016/j.cam.2013.12.007.

[5] B.N. Kim, K. Nah, C. Chu, S.U. Ryu, Y.H. Kang, Y. Kim, Optimal control strategy of plasmodium vivax malaria transmission in Korea, Osong Public Health Res. Perspect. 3 (2012), 128–136. https://doi.org/10.1016/j.phrp.2012.07.005.

[6] O. Prosper, N. Ruktanonchai, M. Martcheva, Optimal vaccination and bednet maintenance for the control of malaria in a region with naturally acquired immunity, J. Theor. Biol. 353 (2014), 142–156. https://doi.org/10.1016/j.jtbi.2014.03.013.

[7] E. Jung, S. Lenhart, Z. Feng, Optimal control of treatments in a two-strain tuberculosis model, Discr. Contin. Dyn. Syst. - B. 2 (2002), 473–482. https://doi.org/10.3934/dcdsb.2002.2.473.

[8] D.P. Moualeu, M. Weiser, R. Ehrig, et al. Optimal control for a tuberculosis model with undetected cases in cameroon, Commun. Nonlinear Sci. Numer. Simul. 20 (2015), 986–1003. https://doi.org/10.1016/j.cnsns.2014.06.037.

[9] T. Rawson, T. Brewer, D. Veltcheva, et al. How and when to end the COVID-19 lockdown: an optimization approach, Front. Public Health 8 (2020), 262. https://doi.org/10.3389/fpubh.2020.00262.

[10] L. Matrajt, J. Eaton, T. Leung, E.R. Brown, Vaccine optimization for COVID-19: who to vaccinate first?, Sci. Adv. 7 (2021), eabf1374. https://doi.org/10.1126/sciadv.abf1374.

[11] A. Rachah, D.F.M. Torres, Mathematical modelling, simulation, and optimal control of the 2014 Ebola outbreak in west Africa, Discr. Dyn. Nat. Soc. 2015 (2015), 842792. https://doi.org/10.1155/2015/842792.

[12] E. Jung, S. Iwami, Y. Takeuchi, T.C. Jo, Optimal control strategy for prevention of avian influenza pandemic, J. Theor. Biol. 260 (2009), 220–229. https://doi.org/10.1016/j.jtbi.2009.05.031.

[13] Y. Su, D. Sun, Optimal control of anti-HBV treatment based on combination of traditional chinese medicine and western medicine, Biomed. Signal Process. Control 15 (2015), 41–48. https://doi.org/10.1016/j.bspc.2014.09.007.

[14] J. Lowden, R. Miller Neilan, M. Yahdi, Optimal control of vancomycin-resistant enterococci using preventive care and treatment of infections, Math. Biosci. 249 (2014), 8–17. https://doi.org/10.1016/j.mbs.2014.01.004.

[15] S. Zouhri, S. Saadi, M. Rachik, Simulating the tumor growth with cellular automata models, Int. J. Computer Appl. 108 (2014), 5–11.

[16] S. Zouhri, S. Saadi, M. Rachik, Simulation of tumor response to immunotherapy using a hybrid cellular automata model, Int. J. Appl. Comput. Math. 3 (2017), 1077–1101. https://doi.org/10.1007/s40819-016-0163-x.

[17] S. Zouhri, M. EL baroudi, S. Saadi, Agent-based model for proteins interaction inside cancer cell, Amer. J. Comput. Appl. Math. 11 (2021), 42-50.

[18] O. Zakary, M. Rachik, I. Elmouki, On the analysis of a multi-regions discrete sir epidemic model: an optimal control approach, Int. J. Dyn. Control 5 (2017), 917–930. https://doi.org/10.1007/s40435-016-0233-2.

[19] O. Zakary, A. Larrache, M. Rachik, et al. Effect of awareness programs and travel-blocking operations in the control of hiv/aids outbreaks: a multi-domains sir model, Adv. Differ. Equ. 2016 (2016), 169. https://doi.org/10.1186/s13662-016-0900-9.

[20] X. Tian, R. Xu, N. Bai, et al. Bifurcation analysis of an age-structured SIRI epidemic model, Math. Biosci. Eng. 17 (2020), 7130–7150. https://doi.org/10.3934/mbe.2020366.

[21] L.S. Pontryagin, Mathematical theory of optimal processes, Routledge, New York, 2018.

[22] S. Lenhart, J.T. Workman, Optimal control applied to biological models, Chapman and Hall/CRC, 2007. https://doi.org/10.1201/9781420011418.

[23] S. Zouhri, M. El Baroudi, Mathematical formalism for agent-based model of proteins interaction inside cancer cell, Commun. Math. Biol. Neurosci. 2023 (2023), 38. https://doi.org/10.28919/cmbn/7720.

[24] S. Zouhri, M. El Baroudi, S. Saadi, Optimal control with isoperimetric constraint for chemotherapy of tumors, Int. J. Appl. Comput. Math. 8 (2022), 215. https://doi.org/10.1007/s40819-022-01425-y.

[25] S. Zouhri, M. El Baroudi, Free end-time optimal control problem for cancer chemotherapy, Differ. Equ. Dyn. Syst. (2023). https://doi.org/10.1007/s12591-023-00654-x.

[26] M. El Baroudi, H. Laarabi, S. Zouhri, et al. Stochastic optimal control model for COVID-19: mask wearing and active screening/testing, J. Appl. Math. Comput. (2024). https://doi.org/10.1007/s12190-024-02220-2.